Failure Mechanisms of Lead Zirconate Titanate Thin Films during Electromechanical Loading

Kathleen Coleman
Materials Science and Engineering Dept. & Materials Research Institute
Pennsylvania State University
University Park, PA,USA
kpc8@psu.edu

Julian Walker
Department of Materials Science and Engineering
Norwegian University of Science and Technology
Trondheim, Norway
julian.walker@ntnu.no

Wanlin Zhu
Materials Science and Engineering Dept. & Materials Research Institute
Pennsylvania State University
University Park, PA,USA
wuz14@psu.edu

Song Won Ko
Xaar Plc & Materials Research Institute
Pennsylvania State University,
University Park, PA,USA
swk10@psu.edu

Peter Mardilovich
Xaar Plc
Cambridge, UK
Peter.Mardilovich@xaar.com

Susan Trolier-McKinstry
Materials Science and Engineering Dept. & Materials Research Institute
Pennsylvania State University
University Park, PA,USA
set1@psu.edu

***Abstract*— Understanding the failure mechanisms of piezoelectric thin films is critical for the commercialization of piezoelectric microelectromechanical systems. This paper describes the failure of 0.6 µm lead zirconate titanate (PZT) thin films on Si wafers with different in-plane stresses under large electric fields. The films failed by a combination of cracking and thermal breakdown events. It was found that the crack initiation and propagation behavior varied with the stress state of the films. The total stress required for crack initiation was estimated to be near 500 MPa. As expected, cracks propagated perpendicular to the maximum tensile stress direction. Thermal breakdown events and cracks were correlated, suggesting coupling between electrical and mechanical failure. It was also found that films that were released from the underlying substrates were less susceptible to failure by cracking. It was proposed that during electric field loading the released film stacks were able to bow and alleviate some of the stress. Released films may also experience enhanced domain wall motion that increases their fracture toughness. The results indicate that both applied stress and clamping conditions play important roles in the electromechancial failure of piezoelectric thin films.**

Keywords—electromechanical failure, lead zirconate titanate, piezoelectric thin films

I. INTRODUCTION

Piezoelectric microelectromechanical systems (PiezoMEMS) are used in a variety of applications including energy harvesters, actuators, sensors, and piezoelectric micromachined ultrasound transducers (PMUT) [1]–[3]. In many of these applications, the piezoelectric thin films are subjected to severe electromechanical loading conditions to achieve high power outputs, signal strengths, and device efficiencies. In sensors and energy harvesters, the mechanical strains applied can be large, and for thin film actuators, the applied electric fields are usually much larger than those experienced by their bulk counterparts [4]–[6]. Electromechanical failure of piezoelectric thin films is thus common and a topic of considerable technological and commercial significance.

Previous failure studies of lead zirconate titanate (PZT) thin films under applied electric fields (E) indicate that the onset of failure is often marked by crack initiation and propagation [7]–[10]. Electric-field induced cracking is believed to be a result of piezoelectric stress (σ_p), which is directly related to the piezoelectric coefficient, $e_{31,f}$, as shown in Equation (1).

$$\sigma_p = -e_{31,f} E \quad (1)$$

Equation (1) points out a fundamental dilemma for piezoMEMS engineers; while a larger $e_{31,f}$ is desirable for increased device output and efficiency, a larger $e_{31,f}$ also results in larger σ_p at a given field.

Since piezoelectric thin films are under large amounts of stress as deposited, several studies have attempted to quantify the total stresses required for crack initiation and propagation [9]–[11]. For PZT thin films, cracks will initiate between approximately 0.5 to 1 GPa [11]. This is a considerably larger stress requirement than for bulk PZT, in which both tensile and bending strength is reach around 50-100 MPa [12], [13]. However, a recent study showed that the crack initiation stress in PZT films depends on the film's thickness [14]. Films that are thicker need less stress for failure [14], [15], due to an energy criterion, which states the required energy in the system (potential energy and work on the system) needs to exceed the surface energy required for creating a

This manuscript is based on work supported by the National Science Foundation, as part of the Center for Dielectrics and Piezoelectrics under Grant Nos. IIP-1361571, IIP-1361503, IIP 1841453, and IIP1841466.

978-1-7281-6430-4/20/$31.00 ©2020 IEEE

Authorized licensed use limited to: Penn State University. Downloaded on April 21,2021 at 17:53:48 UTC from IEEE Xplore. Restrictions apply.

crack [15]. As a result, thin films require high stresses to initiate a crack.

To determine the crack initiation stress of a PZT film, the piezoelectric, residual, and applied stresses must be considered in the total stress calculation. The residual stress is determined by the synthesis method, heat treatments, and substrates used. The substrate typically induces biaxial stress in the film due to thermal expansion mismatch between the substrate and the film [16]–[19]. In this study, uniaxial strains were applied by bending cantilevers [20], resulting in different in-plane x and y stress states, which should lead to anisotropy in the cracking and failure pattern. In addition, the influence of micromachining to remove the underlying substrate on the electromechanical failure was also investigated.

II. Experimental Procedure

$Pb_{0.99}(Zr_{0.52}Ti_{0.48})_{0.98}Nb_{0.02}O_3$ films were made through chemical solution deposition on $LaNiO_3/SiO_2/Si$ wafers (Nova Electronics materials, <001> 500 µm Si with 1 µm thermal oxide) [20]. The films were 0.6 µm thick, with preferred {001} orientations due to the $LaNiO_3$ bottom electrode and seed layers. Further synthesis details are given in [20]. The films all had blanket bottom electrodes and circular top electrodes of sputter deposited Pt, with diameters of 600 µm defined by a lift-off process. During testing, the top electrodes were electrically grounded and the voltage was applied through the bottom electrode.

To drive the films to electromechanical failure, DC electric fields of 500 kV/cm (30 V) were applied while monitoring the leakage current using a Hewlett Packard pA meter. Between 100 and 300 s after the field was applied, the film would fail. The failure was marked by the appearance of black marks produced by localized thermal breakdown, accompanied by spikes in the leakage current and audible electrical arcing between the top and bottom electrodes.

Additional films were subjected to both 500 kV/cm electric fields and applied uniaxial strains (-0.05% to 0.05%). The magnitude of the applied strain was measured using a strain gauge and was varied by changing the force applied to the free end of PZT cantilevers, as described elsewhere [20]. The uniaxial strains were applied down the length of the cantilever (y direction), and the stresses in the x- and y direction were calculated.

III. Results and Discussions

The observed failure patterns seen on the electrodes of the films changed significantly as a function of this applied uniaxial strain (Fig. 1). The thermal breakdown events were visible as small black dots decorating the cracks.

The failure pattern of cracks and thermal breakdown events changed with the direction of the uniaxial applied strain. The cracks propagated predominantly perpendicular to the maximum tensile stress direction, as expected. For example, the electrode in Fig. 1(a) was under a uniaxial compressive strain in the y direction and the maximum tensile stress of 510 ± 50 MPa occurred in the x direction, and so cracks propagate in the y direction. As the uniaxial strain in the y direction was first reduced and then altered to tensile strains, the crack pattern changes to a random crack pattern (Fig. 1(c)) and then cracks align in the x direction (Fig. 1 (d), (e), (f)). The percentage of cracks that aligned within 45° degrees of the maximum tensile strains' direction were above 80% for all the samples. Thus, even the smaller applied strains induced significant orientation of the cracks.

Inspection of the failed films using scanning electron microscopy (SEM) revealed that the electrical and mechanical failures were correlated in time and space (Fig. 2). The debris on the film surfaces is the residue from thermal breakdown events, material expelled violently during breakdown. Both cracks, indicated by arrows, and thermal breakdown events, seen as oval and circular dark features with lighter outer regions of melted material, are clearly present. It is notable that the thermal breakdown events are connected through cracks. It is likely that cracks appear both before and after thermal breakdown. Some of the cracks propagate through the thermal breakdown events, suggesting that the thermal breakdown events occurred first (yellow dashed arrows). In other regions, the thermal breakdown events and the melt region appear on top of the crack, suggesting that the crack occurred first, as indicated by the orange arrow. The order of these mechanisms should depends on when the criteria for each event is met [14], [15], [21], [22]. However, since these two-failure mechanisms are consistently present and the order of events can vary within a single film, it is reasonable to suggest that a single event can cause the other to occur. That is, a thermal breakdown event can initiate cracks by creating sufficient stress and cracks can

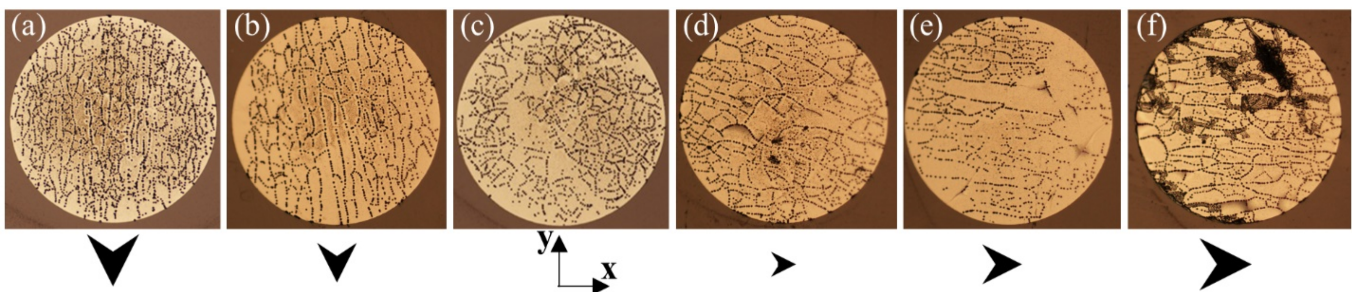

Fig. 1. Optical images of the failure behavior of 600 µm diameter Pt electrodes on 0.6 µm PZT thin films. The electrodes were under -0.051% (a), -0.036% (b), 0.00% (c), 0.02% (d), 0.03% (e), and 0.051% (f) uniaxial strain in the y direction. The arrows represent the direction perpendicular to the maximum tensile stress direction, which also indicates the cracking direction. The larger arrows represent a larger magnitude of the tensile stress. Thermal breakdown events (black dots) decorate the cracks, giving distinct failure patterns based on the applied uniaxial strains.

Authorized licensed use limited to: Penn State University. Downloaded on April 21,2021 at 17:53:48 UTC from IEEE Xplore. Restrictions apply.

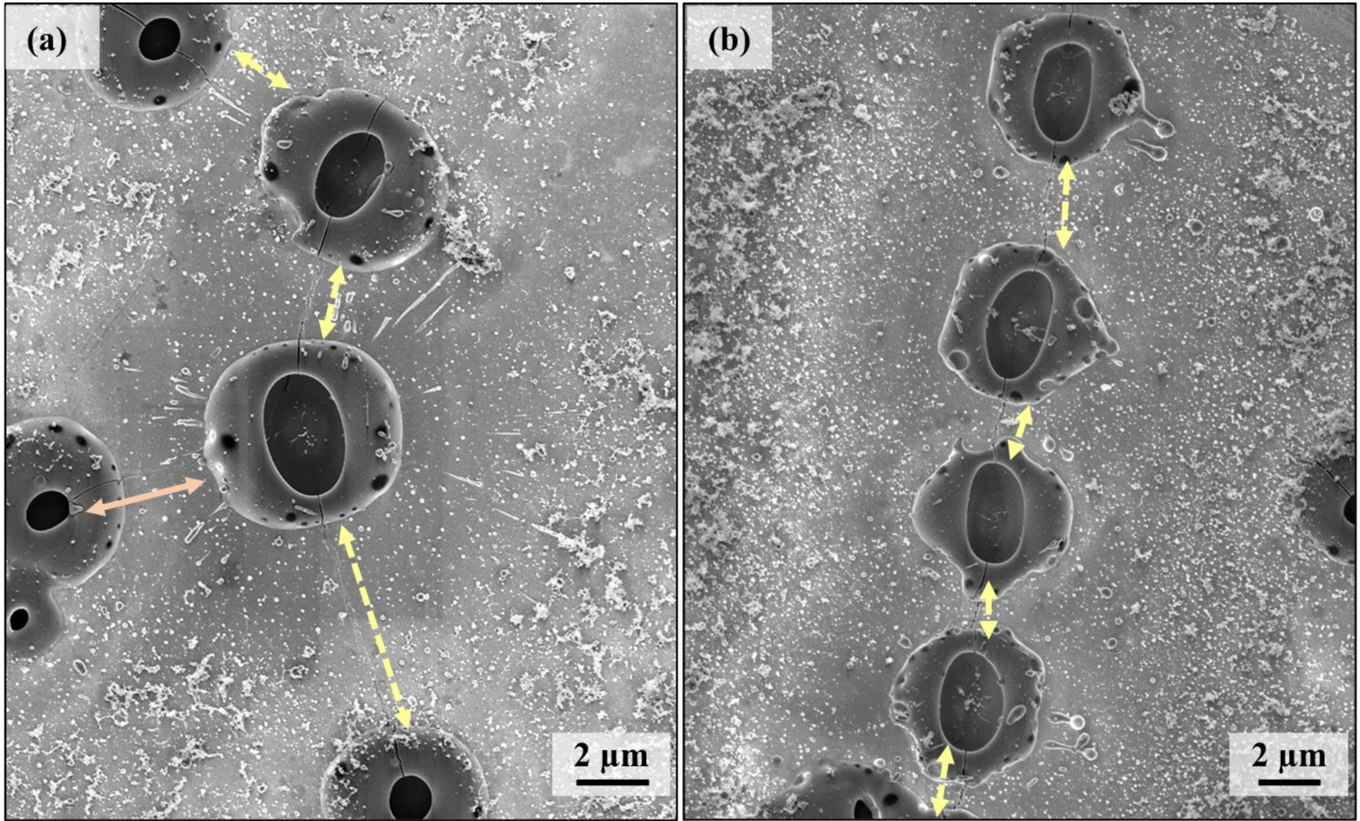

Fig. 2. SEM of the top surface a failed capacitor, showing both crack and thermal breakdown events for a PZT film under 0% applied strain (a), and -0.05% uniaxial strain (b). Cracks connect the thermal breakdown events as shown by the arrows. The yellow dashed arrows represent cracks that would have occurred after the thermal breakdown events as the crack cuts through the thermal breakdown event and the solid orange arrow represents a crack that occurred before the breakdown events it connects. The crack propagates perpendicular to the maximum tensile stress direction as shown in (b).

initiate thermal breakdown events [23] by creating conductive pathways through the film.

To determine the crack initiation criteria for these films, the total stress in the sample was calculated in the in-plane x and y directions, as shown in **Table 1**. The total stress included the residual stress σ_r [20], applied stress σa, and the piezoelectric stress, σ_p, where $e_{31,f}$ was -7.1 C/m^2 for films on Si [20]. With no applied strain and an applied electric field, the PZT samples cracked under a total stress of approximately ~480 MPa. This total stress was slightly lower than the stress required to initiate cracking in PZT thin films with similar thickness under pure mechanical loading [14], but similar to values for films under electromechancial loads [24]. The slight reduction in total stress required for crack initiation may be due to the estimation of the piezoelectric stress in the film. It is assumed that this is solely due to the piezoelectric response of the film described in Equation (1), and it is assumed that the piezoelectric stress is constant. However, the $e_{31,f}$ is a function of both the applied field [25] and stress [20], [26], leading to an underestimation of the total stress of the film here. A second

Table 1. Calculated stresses and crack spacing (δ_c) in the x and y direction for films represented in Fig. 2 (a-f). For σ_p, the piezoelectric coefficient, $e_{31,f}$ was estimated to be -7.1±0.35 C/m^2. Numbers in bold indicate the maximum tensile stress for the sample. To calculate the applied stress in the x ($\sigma_{a,x}$) direction the Poisson's ratio of 0.3, and Young's modulus of 90 GPa for (001) oriented PZT was used [34]. Values are in MPa unless otherwise noted.

Electrode	σ_r	σ_p	$\sigma_{a,y}$	$\sigma_{a,x}$	$\sigma_{tot,y}$	$\sigma_{tot,x}$	δ_c (µm)
a	130 ± 30	350 ± 20	-45	14	455	**514**	21 ± 2.8
b	130 ± 30	350 ± 20	-32	10	468	**510**	26 ± 4.2
c	130 ± 30	350 ± 20	0	0	**480**	**480**	26 ± 2.7
d	130 ± 30	350 ± 20	18	-5	**518**	495	24 ± 3.6
e	130 ± 30	350 ± 20	27	-8	**527**	492	28 ± 6.6
f	130 ± 30	350 ± 20	46	-14	**546**	485	21 ± 3.5

Authorized licensed use limited to: Penn State University. Downloaded on April 21,2021 at 17:53:48 UTC from IEEE Xplore. Restrictions apply.

possible contribution to the reduction in the crack initiation when an electric field is present may be due to a reduction in domain wall motion. The electric field acts to align the polarization, and so may reduce stress-induced ferroelastic switching, which is a toughening mechanism in ferroelectric materials [27], [28].

When the electrodes fail, they consistently have multiple cracks. According to the coupled criterion, with a large energy stored in a material, a long initial crack should be initiated. However, for thin films, this initial crack length may be larger than the thickness of the film and the excess energy will allow for the formation of multiple cracks [29], [30]. It has been reported that films will have smaller crack spacing if they are under more stress, since there is more energy released [29]–[31]. The crack spacing for each sample was calculated in Table 1 using a line intercept method. Lines of various lengths were drawn in the maximum tensile stress direction (or random directions when there was no maximum) and the number of cracks that intercepted the line were counted to determine the crack spacing. The crack spacing was consistent for all samples despite the slight changes in stress (480 to 546 MPa). The small changes in the stress may not be significant enough to induce significant changes in crack spacing.

However, the total area of the electrode that had failed increased with applied stress. The failed surface area was determined using binary images of the electrode in ImageJ®, where the blackened areas were considered to have undergone failure. Those samples subjected to higher levels of applied uniaxial strain, that **is** Fig. 1 (a), (b), and (f), showed that more than 20% of the electrode area had failed. The samples subjected to lower levels of applied strains, Fig. 1 (c), (d), and (e), showed that less than 20% of the electrode area had failed. This difference in failed area may suggest that there is some correlation between the total stress and the energy in the system with the failure behavior.

PZT films clamped to Si substrate are under significant amounts of residual stress and fail mechanically once a threshold stress has been induced. It is notable that films which are released from the substrate may have higher piezoelectric properties due to reduction in the residual stress and increases in domain wall motion [32], [33]. If the residual stress is reduced, then released films may be less prone to cracking for a given applied electric field than a clamped film. Moreover, an increase in domain wall motion may improve the released film's fracture toughness and increase the crack initiation stress.

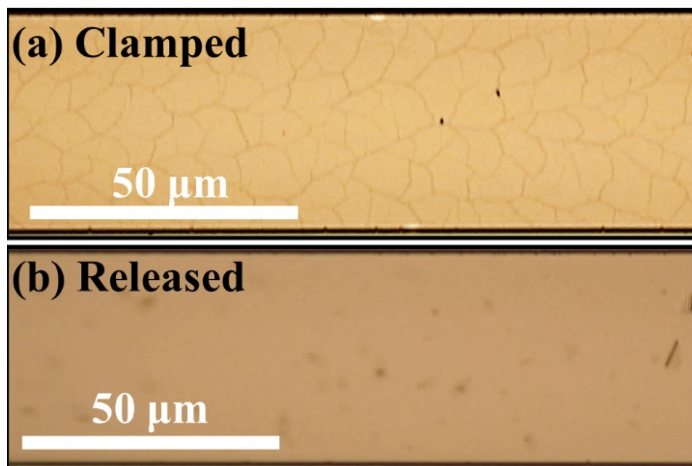

Fig. 3. Observed top electrode after samples have been driven at 733 kV/cm for released device and 785 kV/cm for clamped device. Cracking of the top electrode was observed for PZT films that were clamped (a) and released (b). Cracking was not observed for the released film, but seen on the clamped film in (a).

To explore these possibilities, a series of additional 1.9 μm PZT films that were released from their Si wafer were tested. The term "released" means that the Si wafer beneath the bottom electrode was etched away so that the film stack consists of top electrode, film, bottom electrode, and passive elastic layer. These PZT films were obtained from Xaar. They were prepared by chemical solution deposition and had an MPB composition, so their mechanical properties were expected to be consistent with the previously discussed films. These samples had a DC field applied for 15 s and the amplitude of the DC field was increased by 10 V (52.5 kV/cm) using a 4140B pA meter and Trek2210 voltage amplifier, from 0 to 200 V. The field was held for 3 s prior to an additional increase. The DC signal was driven from the bottom electrode of the released and clamped samples. Above 700 kV/cm both samples failed. The clamped samples shorted at 785 kV/cm and Fig. 3(a) shows the failed electrode where cracking is observed on the surface. Fig. 3(b) shows the electrode for the released film after it shorted at 733 kV/cm. The released film does not show any signs of cracking. Films released from rigid substrates had a reduced propensity for cracking, perhaps due to bowing that relieved piezoelectric stress during electrical loading. This may also be true for PZT films grown on flexible substrates.

IV. Conclusions

The observed failure of PZT films has been shown to depend on both applied strain direction and clamping characteristics. Cracking can be observed when the total stress reaches the crack initiation stress of the film and leads to crack propagation perpendicular to the maximum tensile stress direction. Failure under electromechanical loading conditions was observed as a combination of thermal breakdown events and cracks in films clamped to a Si substrate. To reduce cracking, films should be released from the substrate so they can bow under applied electric fields and withstand higher fields.

Acknowledgment

This manuscript is based on work supported by the National Science Foundation, as part of the Center for Dielectrics and Piezoelectrics under Grant Nos. IIP-1361571, IIP-1361503, IIP 1841453, and IIP1841466. Support from Xaar plc is also gratefully acknowledged.

Authorized licensed use limited to: Penn State University. Downloaded on April 21,2021 at 17:53:48 UTC from IEEE Xplore. Restrictions apply.

REFERENCES

[1] P. Muralt, R. G. Polcawich, and S. Trolier-McKinstry, "Piezoelectric thin films for sensors, actuators, and energy harvesting," *MRS Bull.*, vol. 34, no. September, pp. 658–664, 2009.

[2] N. Izyumskaya, Y. I. Alivov, S. J. Cho, H. Morkoç, H. Lee, and Y. S. Kang, "Processing, structure, properties, and applications of PZT thin films," *Crit. Rev. Solid State Mater. Sci.*, vol. 32, no. 3–4, pp. 111–202, 2007.

[3] C. B. Eom and S. Trolier-McKinstry, "Thin-film piezoelectric MEMS," *MRS Bull.*, vol. 37, no. 11, pp. 1007–1017, 2012.

[4] H. G. Yeo, X. Ma, C. Rahn, and S. Trolier-McKinstry, "Efficient piezoelectric energy harvesters utilizing (001) textured bimorph PZT films on flexible metal foils," *Adv. Funct. Mater.*, vol. 26, no. 32, pp. 5940–5946, 2016.

[5] S. G. Kim, S. Priya, and I. Kanno, "Piezoelectric MEMS for energy harvesting," *MRS Bull.*, vol. 37, no. 11, pp. 1039–1050, 2012.

[6] S. Priya *et al.*, "A review on piezoelectric energy harvesting: materials, methods, and circuits," *Energy Harvest. Syst.*, vol. 4, no. 1, pp. 3–39, 2017.

[7] W. Zhu *et al.*, "Influence of PbO content on the dielectric failure of Nb doped {100} oriented lead zirconate titanate films," *J. Am. Ceram. Soc.*, vol. 102, no. 4, pp. 1734–1740., 2018.

[8] T. M. Borman, W. Zhu, K. Wang, S. W. Ko, P. Mardilovich, and S. Trolier-McKinstry, "Effect of lead content on the performance of niobium-doped {100} textured lead zirconate titanate films," *J. Am. Ceram. Soc.*, no. March, pp. 3558–3567, 2017.

[9] H. D. Chen, K. Udayakumar, K. K. Li, C. J. Gaskey, and L. E. Cross, "Dielectric breakdown strength in sol-gel derived PZT thick films," *Integr. Ferroelectr.*, vol. 15, pp. 89–98, 1997.

[10] Z. Luo, S. Pojprapai, J. Glaum, and M. Hoffman, "Electrical fatigue-induced cracking in lead zirconate titanate piezoelectric ceramic and its influence quantitatively analyzed by refatigue method," *J. Am. Ceram. Soc.*, vol. 95, no. 8, pp. 2593–2600, 2012.

[11] A. Mazzalai, D. Balma, N. Chidambaram, P. Muralt, L. Colombo, and T. Schmitz-Kempen, "Dynamic and long-time tests of the transverse piezoelectric coefficient in PZT thin films," *IEEE Int. Symp. Appl. Ferroelectr. Proc.*, pp. 1–4, 2014.

[12] T. Fett, D. Munz, and G. Thun, "Bending strength of a PZT ceramic under electric fields," *J. Eur. Ceram. Soc.*, vol. 23, no. 2, pp. 195–202, 2003.

[13] D. Munz, T. Fett, S. Mueller, and G. Thun, "Deformation and strength behavior of a soft PZT ceramic," *SPIE Proc. Math. Control Smart Struct.*, vol. 3323, pp. 84–95, 1998.

[14] K. Coleman, R. Bermejo, D. Leguillon, and S. Trolier-McKinstry, "Thickness dependence of crack initiation and propagation in piezoelectric microelectromechanical stacks," *Acta Mater.*, vol. 191, pp. 245–252, 2020.

[15] D. Leguillon, "Strength or toughness? A criterion for crack onset at a notch," *Eur. J. Mech. A/Solids*, vol. 21, no. 1, pp. 61–72, 2002.

[16] B. A. Tuttle and R. W. Schwartz, "Solution deposition of ferroelectric thin films," *MRS Bull.*, vol. 21, no. June, pp. 49–54, 1996.

[17] M. D. Nguyen *et al.*, "Misfit strain dependence of ferroelectric and piezoelectric properties of clamped (001) epitaxial $Pb(Zr_{0.52},Ti_{0.48})O_3$ thin films," *Appl. Phys. Lett.*, vol. 99, no. 25, p. 252904, 2011.

[18] T. A. Berfield, R. J. Ong, D. A. Payne, and N. R. Sottos, "Residual stress effects on piezoelectric response of sol-gel derived lead zirconate titanate thin films," *J. Appl. Phys.*, vol. 101, no. 2, p. 024102, 2007.

[19] C. B. Yeager, Y. Ehara, N. Oshima, H. Funakubo, and S. Trolier-McKinstry, "Dependence of $e_{31,f}$ on polar axis texture for tetragonal $Pb(Zr_x,Ti_{1-x})O_3$ thin films," *J. Appl. Phys.*, vol. 116, no. 10, p. 104907, 2014.

[20] K. Coleman, J. Walker, T. Beechem, and S. Trolier-McKinstry, "Effects of stresses on the dielectric and piezoelectric properties of $Pb(Zr_{0.52}Ti_{0.48})O_3$ thin films," *J. Appl. Phys.*, vol. 126, no. 034101, p. 034101, 2019.

[21] P. H. Moon, "The theory of thermal breakdown of solid dielectrics," *Trans. Am. Inst. Electr. Eng.*, vol. 50, no. 3, pp. 1008–1021, 1931.

[22] J. J. O'Dwyer, "Chapter 6. thermal breakdown," in *The Theory of dielectric breakdown of solids*, Oxford: Clarendon Press, 1964, pp. 183–205.

[23] R. G. Polcawich *et al.*, "Highly accelerated lifetime testing (HALT) of lead zirconate titanate (PZT) thin films," *IEEE Int. Symp. Appl. Ferroelectr.*, vol. 1, pp. 357–360, 2000.

[24] M. Ritter, K. Coleman, R. Bermejo, and S. Trolier-McKinstry, "Effect of electrical history on the mechanical response of PZT thin films," *Prep.*, 2020.

[25] Z. Qiu *et al.*, "Large displacement vertical translational actuator based on piezoelectric thin films," *J. Micromechanics Microengineering*, vol. 20, p. 075016, 2010.

[26] M. A. Dubois and P. Muralt, "Measurement of the effective transverse piezoelectric coefficient $e_{31,f}$ of AlN and $Pb(Zr_x,Ti_{1-x})O_3$ thin films," *Sensors Actuators, A Phys.*, vol. 77, no. 2, pp. 106–112, 1999.

[27] R. Bermejo, H. Grünbichler, J. Kreith, and C. Auer, "Fracture resistance of a doped PZT ceramic for multilayer piezoelectric actuators: Effect of mechanical load and temperature," *J. Eur. Ceram. Soc.*, vol. 30, no. 3, pp. 705–712, 2010.

[28] Y. H. Seo, A. Benčan, J. Koruza, B. Malič, M. Kosec, and K. G. Webber, "Compositional dependence of R-curve behavior in soft $Pb(Zr_{1-x}Ti_x)O_3$ ceramics," *J. Am. Ceram. Soc.*, vol. 94, no. 12, pp. 4419–4425, 2011.

[29] D. Leguillon and E. Martin, "Prediction of multi-cracking in sub-micron films using the coupled criterion," *Int. J. Fract.*, vol. 209, no. 1–2, pp. 187–202, 2018.

[30] D. Leguillon, J. Li, and E. Martin, "Multi-cracking in brittle thin layers and coatings using a FFM model," *Eur. J. Mech. A/Solids*, vol. 63, pp. 14–21, 2017.

[31] N. E. Jansson, Y. Leterrier, and J. A. E. Månson, "Modeling of multiple cracking and decohesion of a thin film on a polymer substrate," *Eng. Fract. Mech.*, vol. 73, no. 17, pp. 2614–2626, 2006.

[32] T. Liu, M. Wallace, S. Trolier-McKinstry, and T. N. Jackson, "High-temperature crystallized thin-film PZT on thin polyimide substrates," *J. Appl. Phys.*, vol. 122, no. 16, 2017.

[33] L. M. Denis, G. Esteves, J. Walker, J. L. Jones, and S. Trolier-McKinstry, "Thickness dependent response of domain wall motion in declamped {001} $Pb(Zr_{0.3}Ti_{0.7})O_3$ thin films," *Acta Mater.*, vol. 151, pp. 243–252, 2018.

[34] D. Das *et al.*, "Control of mechanical response of freestanding $PbZr_{0.52}Ti_{0.48}O_3$ films through texture," *Appl. Phys. Lett.*, vol. 109, no. 13, p. 131905, 2016.

Authorized licensed use limited to: Penn State University. Downloaded on April 21,2021 at 17:53:48 UTC from IEEE Xplore. Restrictions apply.